

## Artocarpol A, a Novel Constituent with Potent Anti-inflammatory Effect, Isolated from *Artocarpus rigida*

by Mei-Ing Chung, Horng-Huey Ko, Ming-Hong Yen, and Chun-Nan Lin\*

School of Pharmacy, Kaohsiung Medical University, Kaohsiung, Taiwan 807, Republic of China

and Sheng-Zehn Yang

Department of Forest Resource, Management and Technology, National Pingtung University of Science and Technology, Ping Tung Hsien, Taiwan 912, Republic of China

and Lo-Ti Tsao and Jih-Pyang Wang

Department of Education and Research, Taichung Veterans General Hospital, Taichung, Taiwan 407, Republic of China

---

A novel phenolic compound, artocarpol A (**1**), was isolated from the root bark of *Artocarpus rigida* and its structure determined by spectroscopic methods and by comparison with its diacetate derivative. Compound **1** strongly inhibited superoxide formation in phorbol 12-myristate 13-acetate (PMA) stimulated rat neutrophils in a concentration-dependent manner with an  $IC_{50}$  value of  $13.7 \pm 0.7 \mu\text{M}$ . Compound **1** also showed a significant inhibitory effect on tumor necrosis factor- $\alpha$  (TNF- $\alpha$ ) formation in lipopolysaccharide(LPS)-stimulated RAW 264.7 cells.

---

**1. Introduction.** – Various constituents isolated from the bark of *Artocarpus rigida* (Moraceae) have been reported [1][2]. Within the scope of our search for biologically active compounds from Formosan *Artocarpus* plants, we investigated the constituents of the root bark of *A. rigida*. The root barks of *A. rigida* were collected at Ping-Tung Hsien, Taiwan, R.O.C., during July 1998. The  $\text{CHCl}_3$  extract was chromatographed (silica gel) and yielded artocarpol A (**1**). In the present paper, the structural characterization, configuration, and anti-inflammatory activity of **1** are reported.

**2. Results and Discussion.** – Compound **1** was isolated as colorless needles. High-resolution MS revealed a  $M^+$  at  $m/z$  444.2394, which corresponds to the molecular formula  $\text{C}_{29}\text{H}_{32}\text{O}_4$ . The IR spectrum indicated the presence of OH groups ( $3399 \text{ cm}^{-1}$ ) and aromatic-ring moieties ( $1620$  and  $1593 \text{ cm}^{-1}$ ). The  $^1\text{H-NMR}$  spectrum of **1** (Table 1) showed five aromatic proton signals ( $\delta$  6.51, 6.55, 6.80, 6.99, and 7.42 ppm) and proton signals of a  $\gamma,\gamma$ -dimethylallyl group ( $\delta$  1.64, 1.70, 3.18, and 5.20 ppm). Analysis of  $^1\text{H},^1\text{H-COSY}$ , HMQC, and HMBC data (Fig. 1) of **1** established the partial structures **a** and **b** (see Fig. 1). The  $^1\text{H-NMR}$  spectrum of **1** also showed proton signals of a 'cyclol', i.e. partial structure **c** in Fig. 1 ( $\delta$  0.60, 0.86, 1.27, 1.57, 1.62, 1.75, 2.02, 2.31, 2.45, and 3.01) [3], whose structure was confirmed by  $^1\text{H},^1\text{H-COSY}$ , HMQC, and HMBC (Fig. 1). The connectivities of partial structures **a–c** were deduced from HMBC data, the configurations from NOESY data (Fig. 2), and the structure of **1** was finally established by further  $^1\text{H}$ - and  $^{13}\text{C}$ -NMR and MS data of **1** and of its diacetate

derivative. Consequently, artocarpol A (**1**) was characterized as *rel*-(10a*R*,12a-*S*,12b*R*,13a*R*)-10a,11,12a,12b,13,13a-hexahydro-10a,13,13-trimethyl-2-(3-methylbut-2-enyl)-12*H*-5,10-dioxacyclobuta[*cd*]dibenzo[3,4:6,7]cyclohepta[1,2-*f*]indene-3,7-diol.

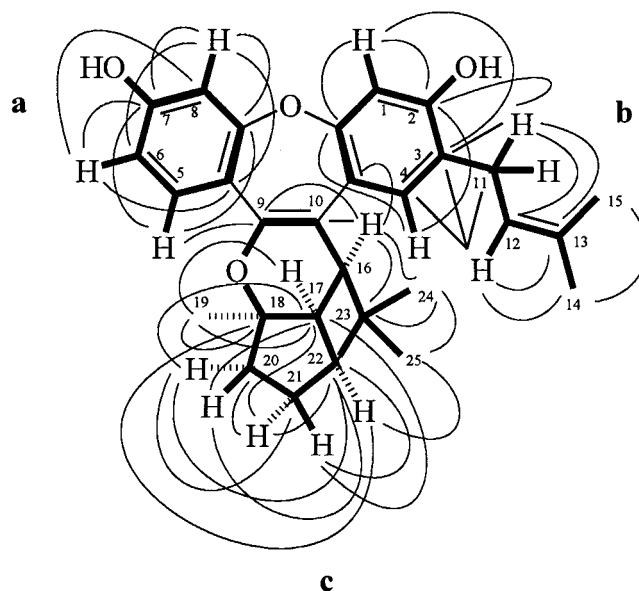


Fig. 1. Structure of **1** and partial structures **a–c** of **1**, with some key HMBC correlations. Bold lines represent  $^1\text{H}, ^1\text{H}$  and  $^1\text{H}, ^{13}\text{C}$  spin systems identified by  $^1\text{H}, ^1\text{H}$ -COSY, HMQC, and HMBC data. Arbitrary numbering.

Table 1.  $^1\text{H}$ - and  $^{13}\text{C}$ -NMR Spectra ( $\text{CDCl}_3$ ) of **1**<sup>a</sup>. Arbitrary numbering according to Fig. 1

	$\delta(\text{C})$	$\delta(\text{H})$		$\delta(\text{C})$	$\delta(\text{H})$
H–C(1)	107.7	6.55 ( <i>s</i> )	H–C(12)	122.6	5.20 ( <i>t</i> , $J=6.8$ )
C(1a)	155.4		C(13)	134.1	
C(2)	153.7		Me(14)	17.8	1.64 ( <i>s</i> )
C(3)	120.5		Me(15)	25.7	1.70 ( <i>s</i> )
H–C(4)	106.5	6.51 ( <i>s</i> )	H–C(16)	38.3	3.01 ( <i>d</i> , $J=9.6$ )
C(4a)	130.7		H–C(17)	40.6	2.45 ( <i>t</i> , $J=9.6$ )
H–C(5)	120.9	7.42 ( <i>d</i> , $J=8.4$ )	C(18)	84.2	
C(5a)	122.3		Me(19)	25.3	1.27 ( <i>s</i> )
H–C(6)	111.8	6.80 ( <i>dd</i> , $J=8.4, 2.4$ )	CH <sub>2</sub> (20)	25.1	1.62 ( <i>m</i> ), 1.75 ( <i>m</i> )
C(7)	153.2 <sup>b</sup> )		CH <sub>2</sub> (21)	41.0	1.57 ( <i>m</i> ), 2.02 ( <i>m</i> )
H–C(8)	98.3	6.99 ( <i>d</i> , $J=2.4$ )	H–C(22)	46.6	2.31 ( <i>dt</i> , $J=8.8, 4.4$ )
C(8a)	153.1 <sup>b</sup> )		C(23)	40.1	
C(9)	153.3 <sup>b</sup> )		Me(24)	19.0	0.60 ( <i>s</i> )
C(10)	119.7		Me(25)	33.3	0.86 ( <i>s</i> )
CH <sub>2</sub> (11)	27.4	3.18 ( <i>d</i> , $J=6.8$ )			

<sup>a</sup>) All assignments were confirmed by HMQC, HMBC, and NOESY data. Chemical shifts  $\delta$  in ppm and coupling constants  $J$  in Hz. <sup>b</sup>) Attributes may be reversed.

In structure **1** (Fig. 1), the HMBC of H–C(5) to C(9) confirmed the connectivity of partial structure **a** to partial structure **c**, and the HMBC of H–C(16) to C(4a) confirmed that the partial structure **c** was linked to partial structure **b** by C(10)–C(4a). In the NOESY experiment with **1**, the correlations between Me(19)/H–C(17)/H<sub>a</sub>–C(20), H<sub>a</sub>–C(20)/H<sub>a</sub>–C(21)/H–C(22), H–C(22)/H–C(16)/H–C(17)/H<sub>a</sub>–C(20), and H–C(16)/H–C(17) (Fig. 2) suggested the  $\alpha$ -configuration for H–C(16), H–C(17), Me(19), and H–C(22). These results and the molecular model of **1** suggested a *trans* arrangement of Me(19) and the geminal Me groups at C(23), and the latter two ( $\delta$  0.60 and 0.86) experienced a positive aryl-shielding contribution [3]. The <sup>1</sup>H-NMR spectrum of the diacetate obtained from **1** showed two acetyl signals at  $\delta$  2.56 (s) and 2.34 (s) and five aromatic-proton signals at  $\delta$  6.61 (s), 6.75 (s), 7.01 (*dd*,  $J = 8.4, 2.4$  Hz), 7.27 (*d*,  $J = 2.4$  Hz) and 7.55 (*d*,  $J = 8.4$  Hz). By comparing the aromatic-proton chemical shifts of **1** (Table 1) and of its diacetate, it was found that the signal at  $\delta$  6.55, 6.80, and 6.99 of **1** experienced a significant downfield shift of  $\Delta\delta = +0.20, +0.21, \text{ and } +0.27$  ppm, respectively, upon acetylation, whereas the signal at  $\delta$  6.51 and 7.42 of **1** showed only a slight downfield shift of  $\Delta\delta = +0.10$  and 0.13 ppm, respectively. In addition to the acetylation-induced shifts [4], **1** showed a negative *Gibb's* test and significant NOESY interactions between a phenol signal at  $\delta$  4.88 (s, 1 H, exchange with D<sub>2</sub>O) and H–C(12), Me(14), and Me(15), thus establishing an ether linkage between C(1a) and C(8a) of partial structures **a** and **b**, respectively (Fig. 1).

The <sup>13</sup>C-NMR spectrum of **1** (Table 1) supported the structure assignment. The base peak at  $m/z$  361 in the MS of **1** was attributed to the fragments  $[429 - b - H]^+$  (Fig. 2). This and characteristic peaks at  $m/z$  429 ( $[M - a]^+$ ), 305 ( $[429 - CO - 3 H]^+$ ), 235 ( $[305 - b - H]^+$ ), and 223 ( $[361 - c - H]^+$ ) (Fig. 2) also confirmed the structure assignment of **1**.

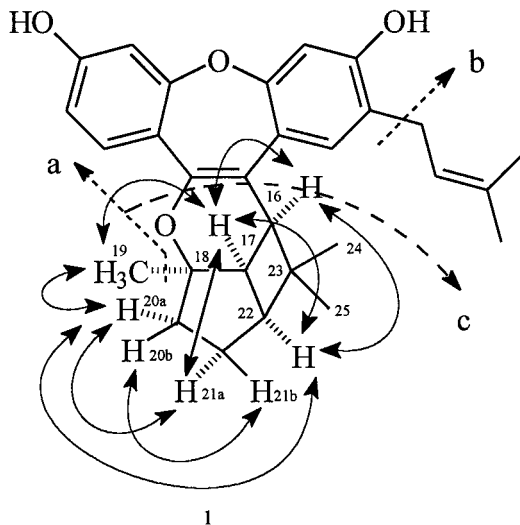


Fig. 2. Some key NOESY interactions and EI-MS fragmentation patterns of **1**

The anti-inflammatory activities of **1** were studied *in vitro* by measuring the inhibitory effects on the chemical mediators released from mast cells, neutrophils, macrophages, and microglial cells. Compound **1** did not cause significant inhibition of mast-cell degranulation stimulated with compound 48/80 and neutrophil degranulation stimulated with formyl-Met-Leu-Phe (fMLP) (1  $\mu$ M)/cytochalasin B (CB) (5  $\mu$ g/ml) (data not shown) [5–7]. fMLP (0.3  $\mu$ M)/CB (5  $\mu$ g/ml) or PMA (3 nM) also induced the superoxide-anion formation from rat neutrophils. As shown in Table 2, **1** strongly inhibited superoxide anion formation in phorbol 12-myristate 13-acetate (PMA) stimulated rat neutrophils in a concentration-dependent manner with an  $IC_{50}$  value of  $13.7 \pm 0.7$   $\mu$ M, while it did not significantly inhibit the superoxide-anion formation from

rat neutrophils stimulated with fMLP/CB (data not shown). The data indicate that fMLP/CB and PMA induce the superoxide-anion formation from rat neutrophils, but that they utilize different transduction mechanisms and are regulated differently [8][9].

Table 2. *The Inhibitory Effect of 1 on Superoxide-Anion Formation from Rat Neutrophils Stimulated with PMA*<sup>a)</sup>

Compound	Superoxide formation	
	$x$ mol/10 <sup>6</sup> cells/30 min	% inhibition
Control	3.14 ± 0.12	
<b>1</b> 1 μM	4.38 ± 0.74	– 37.3 ± 3.0
3 μM	3.55 ± 0.68	– 10.6 ± 7.8
10 μM	0.57 ± 0.03 <sup>b)</sup>	80.7 ± 3.9
30 μM	0.35 ± 0.09 <sup>b)</sup>	88.6 ± 3.2
Trifluoperazine 1 μM	2.55 ± 0.23	16.6 ± 0.1
3 μM	1.59 ± 0.43 <sup>b)</sup>	49.5 ± 7.4
10 μM	0.39 ± 0.19 <sup>b)</sup>	87.1 ± 4.9

<sup>a)</sup> Values are expressed as the means ± s.e.m. ( $n = 3$ ). <sup>b)</sup>  $p < 0.01$  compared with control.

Following the activation of mouse macrophage-like cell line RAW 264.7 and murine microglial cell line N9, NO and TNF- $\alpha$  were generated in response to LPS and LPS/interferon- $\gamma$  (IFN- $\gamma$ ), respectively [10–12]. Compound **1** did not cause significant inhibitory effects on NO accumulation from RAW 264.7 and N9 cells in response to LPS (1 μg/ml) and LPS (10 ng/ml)/IFN- $\gamma$  (10 unit/ml) (data not shown), respectively [13]. Compound **1** (3 μM) caused potent inhibitory effects on the product of TNF- $\alpha$  from RAW 264.7 cells induced by LPS (1 μg/ml) with a % inhibition of 40.1 ± 2.0, while it (1 μM) showed a slight inhibitory effect on the production of TNF- $\alpha$  from N9 cells induced by LPS (10 ng/ml)/IFN- $\gamma$  (10 unit/ml) with a % inhibition of 15.7 ± 1.5. These results indicate that **1** may attenuate the respiratory burst in neutrophils and suppress the TNF- $\alpha$  formation from macrophages.

This work was supported by a grant from the *National Science Council of R.O.C.* (NSC 88-2314-B-037-037).

### Experimental Part

*General.* M.p.: uncorrected. UV Spectra: *Jasco-UV-VIS* spectrophotometer;  $\lambda_{\max}$  (log  $\epsilon$ ) in nm. IR Spectra: *Hitachi 260-30* spectrometer;  $\tilde{\nu}$  in  $\text{cm}^{-1}$ . <sup>1</sup>H- and <sup>13</sup>C-NMR Spectra: *Varian-Unity-400* spectrometer; 400 and 100 MHz, resp.;  $\delta$  in ppm,  $J$  in Hz. MS: *JMS-HX-100* mass spectrometer;  $m/z$  (rel %).

*Plant Material.* Root barks (8.5 kg) of *A. rigida* were collected at Ping-Tung Hsien, Taiwan, in July 1998. A voucher specimen is deposited in the laboratory of medicinal chemistry.

*Extraction and Isolation.* The root barks of *A. rigida* were chipped and extracted with  $\text{CHCl}_3$  at r.t. The extract was subjected to column chromatography (silica gel, cyclohexane/ $\text{CH}_2\text{Cl}_2$ /AcOEt 6:3:1): **1** (150 mg). Colorless needles. M.p. 181–182°.  $[\alpha]_{\text{D}}^{25} = -8$  ( $c = 0.1$ ,  $\text{CHCl}_3$ ). UV (MeOH): 213 (4.45), 297 (4.15), 403 (2.87). IR (KBr): 3399, 1620, 1593. <sup>1</sup>H- and <sup>13</sup>C-NMR: *Table 1*. EI-MS (70 eV; see *Fig. 2*): 444 (20,  $M^+$ ), 429 (6), 361 (100), 317 (5), 305 (15), 277 (9).

*Diacetate of 1.* Amorphous powder.  $[\alpha]_{\text{D}}^{25} = -6$  ( $c = 0.1$ ,  $\text{CHCl}_3$ ). <sup>1</sup>H-NMR ( $\text{CDCl}_3$ , 400 MHz; for numbering, see *Fig. 1*): 0.62 (*s*, Me(24)); 0.88 (*s*, Me(25)); 1.28 (*s*, Me(19)); 1.42 (*s*, Me(14)); 1.57 (*s*, Me(15)); 1.60 (*m*, 1 H–C(21)); 1.66 (*m*, 1 H–C(20)); 1.76 (*m*, 1 H–C(20)); 2.03 (*m*, 1 H–C(21)); 2.35 (*m*, H–C(22)); 2.46 (*t*,  $J = 9.2$ , H–C(17)); 2.26, 2.34 (2 *s*, 2 Ac); 3.01 (*d*,  $J = 9.2$ , H–C(16)); 3.08 (*d*,  $J = 4.8$ , 1 H–C(11)); 4.97

(*t*, *J* = 4.8, H–C(12)); 6.61 (*s*, H–C(4)); 6.75 (*s*, H–C(1)); 7.01 (*dd*, *J* = 8.4, 2.4, H–C(6)); 7.27 (*d*, *J* = 2.4, H–C(8)); 7.55 (*d*, *J* = 8.4, H–C(5)).

**Superoxide-Anion Formation.** Superoxide-anion formation was measured in terms of superoxide dismutase inhibitable cytochrome *c* reduction [14]. Neutrophil suspension was preincubated at 37° with 0.5% DMSO or drugs for 3 min, and then superoxide dismutase of HBSS was added to the blank and test tubes, respectively. The reaction was initiated by challenge with fMLP (0.3 μM)/CB (5 μg/ml) of PMA (3 nM). After 30 min, the reaction was terminated by centrifugation and the absorbance change of supernatants was monitored at 550 nm in a microplate reader. The final concentration of DMSO was fixed at 0.5%.

**Macrophage Cultures and Drugs Treatment.** RAW 264.7 mouse macrophage-like cell line (American Type Culture Collection) was plated in 96-well tissue-culture plates in *Dulbecco's* modified eagle medium supplemented with 5% fetal calf serum (FCS), 100 unit/ml of penicillin and streptomycin at 2 · 10<sup>5</sup> cells/200 μl per well. Cells were allowed to adhere overnight. Pretreatment of cells with test drugs was done at 37° for 1 h before stimulation with 1 μg/ml of LPS (*Escherichia coli*, serotype 0111:B4) for 24 h, and then the medium was collected and stored at –70°C until used. The final concentration of DMSO was fixed at 0.5%.

**Microglial Cell Cultures and Drug Treatment.** Murine microglial cell lines N9 [15] (kindly provided by Dr. P. Ricciardi-Castagnoli, CNR, Cellular and Molecular Pharmacology Center, Italy) was plated in 96-well tissue-culture plates in *Iscove's* modified *Dulbecco's* medium containing 2% heat-inactivated FCS and antibiotics at 8 · 10<sup>4</sup> cells/200 μl per well. Pretreatment of cells with test drugs was done at 37° for 1 h before stimulation with LPS (10 ng/ml/IFN-γ (10 unit/ml)) for 24 h, and then the medium was collected and stored at –70° until used. The final concentration of DMSO was fixed at 0.5%.

**TNF-α Determination.** TNF-α in medium was measured by an *EIA* kit according to the procedure described by the manufacturers.

**Statistical Analysis.** Data are presented as the means ± s.e.m. Statistical analyses were performed with the least-significant-difference test method after analysis of variance. *P* Values < 0.05 were considered to be significant. Analysis of the regression line was used to calculate *IC*<sub>50</sub> values.

#### REFERENCES

- [1] Y. Hano, R. Inami, T. Nomura, *Heterocycles* **1990**, 31, 2173.
- [2] Y. Hano, R. Inami, T. Nomura, *Heterocycles* **1993**, 35, 1341.
- [3] T. Nomura, T. Fukai, M. Katayangi, *Heterocycles* **1978**, 9, 745.
- [4] W. Steglich, W. Losel, *Tetrahedron* **1964**, 25, 4391.
- [5] J. P. Wang, S. L. Raung, C. N. Lin, C. M. Teng, *Eur. J. Pharmacol.* **1994**, 251, 35.
- [6] A. Boyum, *J. Clin. Invest.* **1968**, 97 (Suppl.), 77.
- [7] R. J. Smith, S. S. Iden, *Biochem. Biophys. Res. Commun.* **1979**, 91, 263.
- [8] L. C. Mcphail, R. Snyderman, *J. Clin. Invest.* **1983**, 72, 192.
- [9] F. Morel, J. Doussiere, P. V. Vignais, *Eur. J. Biochem.* **1991**, 210, 523.
- [10] A. H. Ding, C. F. Nathan, D. J. Stuehr, *J. Immunol.* **1988**, 141, 2407.
- [11] L. Meda, M. A. Cassatella, G. I. Szendrei, L. Otvos Jr., P. Baron, M. Villalba, D. Ferrari, F. Ross, *Nature (London)* **1995**, 374, 647.
- [12] B. Beutler, A. Cerami, *Am. Rev. Biochem.* **1988**, 57, 505.
- [13] L. Minghetti, A. Nicolini, E. Polazzi, C. Creminon, J. Maclouf, G. Levi, *Glia.* **1997**, 19, 152.
- [14] M. Market, P. C. Andrews, B. M. Babior, *Methods Enzymol.* **1984**, 105, 358.
- [15] S. B. Corradin, J. Mael, S. D. Donini, E. Quattrocchi, P. Ricciardi-Casagnoli, *Glia.* **1993**, 7, 255.

Received November 29, 1999